AD-A033 923 MISSOURI UNIV-ROLLA F/G 20/8
PENNING IONIZATION: MEASUREMENT OF ION AND MOLECULAR LIFETIMES.(U)
DEC 76 R A ANDERSON, L D SCHEARER N00014-75-C-0477
UNCLASSIFIED NL

1 OF 1
AD A033923

END
DATE FILMED
2 - 77

Penning Ionization: Measurement of Ion & Molecular Lifetimes

L.D. Schearer
R.A. Anderson
University of Missouri - Rolla

Annual Report to the Office of Naval Research
Grant no. N00014 - 75 - c - 0477 for the period Oct. 1975 - Dec. 1976

SECURITY CLASSIFICATION OF THIS PAGE (When Data Entered)

REPORT DOCUMENTATION PAGE	READ INSTRUCTIONS BEFORE COMPLETING FORM
1. REPORT NUMBER: 10 (9) Annual rept. no. 10, 1 Oct 75 - 1 Dec 76	2. GOVT ACCESSION NO. / 3. RECIPIENT'S CATALOG NUMBER
4. TITLE (and Subtitle): Penning Ionization: Measurement of Ion (6) Molecular Lifetimes	5. TYPE OF REPORT & PERIOD COVERED: Annual, October 1, 1975 to December 1, 1976
	6. PERFORMING ORG. REPORT NUMBER
7. AUTHOR(s): (10) R. A. Anderson, L.D. Schearer	8. CONTRACT OR GRANT NUMBER(s): (15) N00014-75-C-0477
9. PERFORMING ORGANIZATION NAME AND ADDRESS: The Curators of the University of Missouri, Rolla, MO 65401	10. PROGRAM ELEMENT, PROJECT, TASK AREA & WORK UNIT NUMBERS: NR 343-011
11. CONTROLLING OFFICE NAME AND ADDRESS: Department of the Navy, Office of Naval Research, Washington, D.C. 20360	12. REPORT DATE: (11) 1 Dec 1976
	13. NUMBER OF PAGES: (12) 37 pp.
14. MONITORING AGENCY NAME & ADDRESS (if different from Controlling Office)	15. SECURITY CLASS. (of this report): Unclassified
	15a. DECLASSIFICATION/DOWNGRADING SCHEDULE

16. DISTRIBUTION STATEMENT (of this Report)

Approved for public release: Distribution unlimited.

9-A019 992

17. DISTRIBUTION STATEMENT (of the abstract entered in Block 20, if different from Report)

18. SUPPLEMENTARY NOTES

19. KEY WORDS (Continue on reverse side if necessary and identify by block number)

Penning ionization, Hanle effect, rotational lifetimes, dye lasers.

TABLE OF CONTENTS:

20. ABSTRACT (Continue on reverse side if necessary and identify by block number)

"Radiative lifetimes and alignment depolarization cross sections for Yb(I) and (II) by the Hanle effect in a flowing helium system"; F.H.K. Rambow and L.D. Schearer, Phys. Rev. A, Vol. 14, No. 2,738 (August, 1976).

"Intense flowing hollow cathode lamp"; F.H.K. Rambow and L.D. Schearer, accepted for publication Rev. Sci Inst. Dec., 1976.

next page

400 144

1 of 2

DD FORM 1 JAN 73 1473 EDITION OF 1 NOV 65 IS OBSOLETE

S/N 0102-LF-014-6601

SECURITY CLASSIFICATION OF THIS PAGE (When Data Entered)

20.

"The Violation of the Franck-Condon Principle in Penning Ionization"; W.F. Parks, Proceedings of 5th International Conference on Atomic Physics, Berkeley, CA July 26-30, 1976.

"Radiative Lifetime of the $A^2\Delta$ State of CH"; James Carozza and Richard Anderson, accepted for publication, J. Chem. Phys., Dec., 1976.

"A High-Power Pulsed Xenon Ion Laser as a Pump Source for a Tunable Dye Laser"; L.D. Schearer, IEEE J. of Quan. Elec., Vol. QE-11, No. 12, Dec. 1975.

"Radiative lifetimes of some group II ions by the Hanle effect in a fast-flowing helium afterglow"; F.H.K. Rambow and L.D. Schearer, Phys. Rev. A, Vol. 14, No. 5, Nov. 1976.

A squared sigma(+)

"Rotational and predissociation lifetimes of the $A^2\Sigma^+$ state of OD;" David Wilcox, Richard Anderson, and Jerry Peacher, J. Opt. Soc. of Amer. Vol 65, 11, 1368 (Nov. 1975).

and "Radiative lifetime of the $B^2\Sigma^-$ state of CH", Richard A. Anderson, Jerry Peacher, and David M. Wilcox, J. of Chem. Phys. Vol. 63, 12, 5287 (Dec. 1975).

B squared sigma(-)

*A squared delta

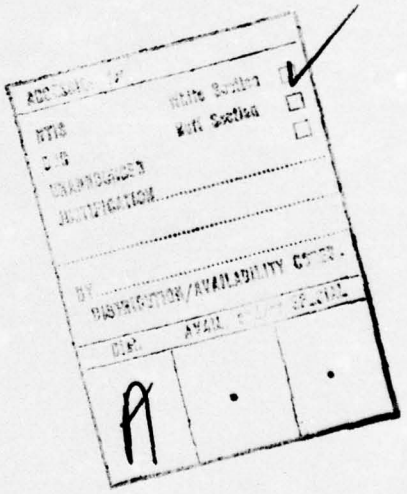

TABLE OF CONTENTS

I. Research Accomplishments

(A) Penning Ionization: Ion Lifetimes

We have been able to demonstrate over the course of this work:

(1) that the Penning ionization process is an efficient mechanism for the production of ions, and in this connection a variety of Penning ionization cross sections were measured.[1]

(2) that the fast flowing helium (argon) afterglow was a particularly valuable tool available for the study of the Penning process and associated experimental observations. This value stems principally from the fact that large steady-state concentrations of both atomic and molecular ions can be obtained in a field-free region without the complications of high vacuum techniques and large volume ovens.[2]

(3) that Penning collisions are a spin-conserving process. Here we have utilized the optical pumping technique in metastable helium which induces a spin orientation in the He^m system.[2] Subsequent Penning collisions of the He^m atoms with Group II metal atoms results in our orientation of the Penning ion. Utilizing these observations in various combinations we have been able to measure a number of radiative lifetimes and collisional depolarization cross sections.[3] Utilizing the flowing system (without, however, the use of Penning ionization) we have also measured by the Hanle method, the radiative lifetimes of a number of excited YbI levels.[4]

NBS is currently preparing a monograph on the properties (energy levels, configurations, etc.) of Yb, and we have both utilized and contributed to their program in this area.

We have also completed the construction of a fast metastable beam source[5] which is to be used in conjunction with the flowing afterglow system. The beam source provides a unique collision axis as opposed to the flowing system in which there is no well-defined collision axis.

As a result of our cross section measurements for the quenching of the metastable states of He, Ne, Ar and Kr by Cd & Zn in Penning ionization collision, we have considered the theoretical models for Penning ionization which are currently in vogue. Some preliminary theoretical observations were presented at the 5th International Conference on Atomic Physics. A more detailed description is being prepared for publication.

(B) Excitation Transfer, Collisional Dissociative Excitation

Collisions of this type are very important mechanisms in certain laser systems in which the noble gas excited atom is the energy carrier and precursor of a dissociative excitation process. Notable are the noble-gas halogen laser excimer systems[6] and the recent report of high power lasing action in neutral atomic fluorine.[7] In this latter system a fast discharge produced dissociation of NF_3 in a mixture of ~100 Torr Helium, 1 Torr NF_3. Lasing was observed at 7000Å with 70 KW obtained in 40 nsec pulses.

In an effort to determine the role of helium in the process we utilized the flowing helium afterglow with SF_6 and F_2 added as an impurity. Intense emission near 7000Å due to emission from atomic fluorine was obtained. We suggest that the internal energy of the He^m is transferred to the molecule resulting in dissociative excitation and the efficient production of electronically excited atomic fluorine. Our results indicate that the use of molecular fluorine may provide greater efficiency than the use of NF_3. Interest in this laser system stems from its possible use as a pump source for infrared dye laser systems.

(C) Xenon Ion Laser as a Pump Source for Tunable Dye Laser

As a result of our need for an inexpensive source of tunable laser radiation we have investigated the use of the Xenon ion laser as a pump source for narrow band tunable laser radiation. A report of our early results was published earlier.[8] Subsequently, we have examined the use of the system with various dyes and are now able to obtain tunable laser radiation from 5500Å to beyond 7000Å with various dyes. The chief advantages of the present systems are: low cost, relatively long pulse (~200-500 nsec) repetition rates to 30 Hz, a bandwidth of 0.25Å with potential for substantial narrowing with the use of an etalon, an 0.3ml sealed dye volume, and up to 10% conversion efficiency.

(D) Molecular Lifetime Measurements

Rotation and predissociation lifetimes of the $A^2\Sigma$ of OD and radiative lifetimes of the $B^2\Sigma$ and $A^2\Delta$ state of CH were obtained.

REFERENCES

1. L.A. Riseberg, W.F. Parks, & L.D. Schearer, Phys. Rev. 8, 1962 (1973).
2. L.D. Schearer, Phys. Rev. 10, 1380 (1974).
3. F.H.K. Rambow & L.D. Schearer, Phys. Rev. 14, 1736 (1976).
4. F.H.K. Rambow & L.D. Schearer, Phys. Rev. 14, 738 (1976).
5. J.Q.Searcy, Rev. Sci. Instrum. 45, 589 (1974).
6. C.P. Wang, H. Mirels, D.G. Sutton & S.N. Suchard, App. Phys. Lett. 28, 326 (1976).
7. Irving J. Bigio & R.F. Begley, App. Phys. Lett 28, 263 (1976).
8. L.D. Schearer, IEEE J. Quant. Elec. 11, 935 (1975).

REPRINTS OF PUBLISHED WORK

PHYSICAL REVIEW A VOLUME 14, NUMBER 2 AUGUST 1976

Radiative lifetimes and alignment depolarization cross sections for Yb I and II by the Hanle effect in a flowing helium system*

F. H. K. Rambow and L. D. Schearer
Physics Department, University of Missouri-Rolla, Rolla, Missouri 65401
(Received 29 March 1976)

The radiative lifetimes of the 17992-, 25068-, 28857-, 37414-, 40564-, and 44017-cm^{-1} neutral levels and the 30392-cm^{-1} ion level of Yb have been measured by the Hanle method in a fast-flowing He system. The lifetimes (in units of 10^{-9} sec) were found to be 820(20), 5.12(0.12), 14.4(0.4), 77.4(6.0), 9.32(0.6), 39.1(3.5), and 5.8(0.6), respectively. In a flowing system with He as a buffer gas the alignment depolarization cross sections with Yb were obtained and are reported here for the first time. They are (in units of 10^{-15} cm^2) 5.0(1.0), 5.9(1.0), 5.9(1.2), 17.9(2.0), 28.2(3.0), 5.16(4.0), and 7.2(2.5), respectively.

INTRODUCTION

Lifetime and depolarization cross sections are important parameters of excited states of atoms. We report here radiative lifetimes and collisional depolarization cross sections for six odd levels of neutral ytterbium and one level of singly ionized ytterbium as measured by the Hanle effect[1] in a flowing system with helium as the buffer gas. The electron configuration of one of these neutral levels (37 414 cm^{-1}) has not yet been identified.[2] Although ytterbium was discovered in 1907, relatively little progress was made towards a quantum description of its spectra until recently, due in part to the difficulty of obtaining pure samples of Yb. Since 1950 more efficient light sources have been developed and relatively large quantities of high-purity rare earths have been accumulated as by-products of the purification of thorium and uranium by ion-exchange chromatography.

A useful description of its arc and spark spectra was first given by Meggers and Scribner in 1937.[3] The first useful Zeeman measurements on Yb I were made in the late 1950's. In 1965 Meggers and Corliss published data for some 7300 spectral lines, including Zeeman classification of 1300 lines.[4] At present a quantum description of Yb I is being prepared for publication by J. Tech at the U. S. National Bureau of Standards.[2] However, the electron configuration of several levels remain unidentified.

We found few reliable lifetime measurements and no depolarization cross sections in the literature for Yb. One of the first lifetime measurements on Yb was that of Baumann and Wandel in 1966.[5] They measured radiative lifetimes for the ^1P and ^3P levels of the $4f^{14}6s6p$ configuration of Yb I by the Hanle effect in a beam. These and all subsequent measurements can be broken roughly into three groups. The longest lifetimes were measured by the technique of anomalous dispersion and total absorption.[6] These averaged 20% longer than measurements in the second group using the Hanle technique and taken by Bauman and Wandel, Lange *et al.*,[7] and ourselves. Also agreeing with these data for the neutrals and included in the second group was the technique of delayed coincidence[8] used by Burshtein *et al.*, which gave a value only slightly longer than that obtained via the Hanle effect. However, their value for the ion lifetime, which incidentally is the first such measurement, is about 20% longer than ours. Possible reasons for this will be discussed later. The third group, also using the Hanle method but as a by-product of level crossing hyperfine studies, was that of Budick and Snir.[9,10] Their values obtained for the $6s6p\,^1P_1$ and $4f^{13}5d6s^2(3\frac{1}{2}, 2\frac{1}{2})^o_1$ levels were 100% and 20% longer, respectively, than those in the second group. Their value for the $6s6p\,^3P_1$ was only slightly shorter than that of the second group. These discrepancies can be explained if coherence narrowing and collisional depolarization were not properly taken into account.

In this experiment we were particularly careful to account for these effects. The data reported here have been corrected for collisional broadening and coherence narrowing. Our measurements of collisional depolarization cross sections are, to our knowledge, the first reported. Furthermore, the fluctuation of a data point over several measurements averaged <2% for the neutral atom due to the large signal-to-noise ratio. The error limits we have set in Table I represent maximum confidence limits but do not take into account hyperfine effects. Scatter of the data lies within these limits in all cases. The influence of nuclear

spin is considered separately.

APPARATUS

The Hanle effect in a flowing system is particularly suited to measurements of lifetimes and depolarization cross sections. It allows for rapid change and easy monitoring of system parameters, such as ytterbium density and buffer-gas pressure. Thus collisional depolarization and radiation trapping can be easily controlled and their effects observed. Another advantage is that material under study can be quickly changed and, unlike a beam apparatus or sealed cells, high-vacuum techniques are not necessary, since flow rates are many orders of magnitude greater than outgassing rates.

The flow tube is welded from aluminum conduit and is evacuated by a mechanical forepump and roots blower combination rated at 540 ft^3/min. With helium admitted at the entrance of the flow tube, flow velocities on the order of 10^3–10^4 cm/sec were obtained with background He pressures in the range of 0.01–1 Torr. The Yb vapor is titrated into the interaction region by an oven wound with coaxial heater wire. The resonance light source is a flowing hollow cathode lamp with a water-cooled anode and air-cooled Pyrex jacket. Resonance emission from the lamp was monitored by a 1-m Jarrell Ash monochromator having a resolution of 0.05 Å. No evidence for broadening or self-reversal of the line profile was observed within this limit.

A schematic diagram of the apparatus is shown in Fig. 1. Light from the flowing hollow cathode is focused by a fused quartz lens through a quartz window into the flow region just above the oven. Magnetic field coils in a Helmholtz configuration are mounted coaxially on the flow tube. Three more sets of Helmholtz coils cancel the Earth's field in the scattering region to less than 10 mG residual field. Light scattered perpendicular to both the incident light direction and the magnetic field is collected and passed through a $\frac{1}{4}$-m Jarrel Ash monochromator with 1000-μm slits to a photomultiplier.

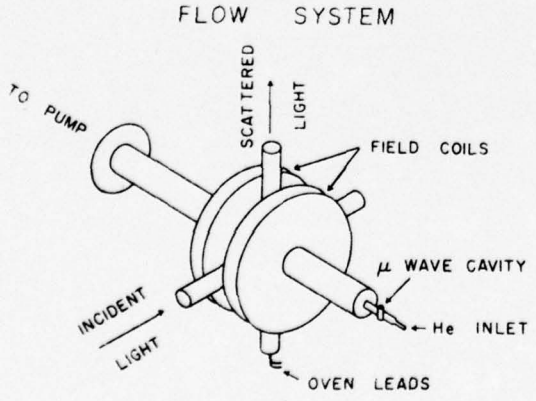

FIG. 1. Schematic diagram of apparatus.

The magnetic field is swept at 18 Hz by a triangular current waveform. The current waveform is shaped by a feedback network that holds the sweep linear to better than 0.5% over the entire waveform. Linearity can be monitored by two methods. One is the helium magnetometer, which is discussed below, and the other is a probe coil inserted into the flow tube. When the voltage induced in this coil is integrated it provides an accurate picture of the magnetic field inside the flow tube. Linear field sweeps of over 100 G peak to peak were obtained.

One of the advantages of performing this experiment with a flowing He system is the *in situ* field calibration it allows. A microwave discharge at the flow inlet produces He metastables which drift down the tube and are optically pumped by light from a flowing He lamp focused just above the oven.[11] A small rf coil provides the oscillating magnetic field to induce the Zeeman transitions. The He light is monitored in transmission by a Polaroid infrared polarizer filter in conjunction with an infrared-sensitive photodiode. This provides not only a calibration of the field but also a check on field sweep linearity. Linearity is defined by measuring the spacing between resonances in gauss for a series of radio frequencies, i.e., 10, 20, . . . , 50 MHz, and dividing the maximum difference in spacing by the average spacing.

This same flowing system was used for Hanle measurements on the ion. With the microwave-excited source of helium metastables (He^m) at the inlet to the flow tube, Penning ionization of Yb by He^m produces copious quantities of ions in steady state in a field-free region. Typical cross sections for Penning ionization are on the order of 10^{-15} cm^2. Resulting ion densities as high as 10^{10} cm^{-3} are estimated by optical absorption. This technique releases one from concerns over perturbations due to an ionizing electric field and decreases necessary signal accumulation time over pulsed techniques.

EXPERIMENTAL TECHNIQUE

Briefly, the Hanle method is a well-known zero-field level-crossing technique in which resonance radiation is used to coherently excite atoms in the presence of a magnetic field. The resonance fluorescence is observed as a function of magnetic field and from this resulting plot the decay constant is obtained as a function of the g factor. We have chosen the common geometry and polarization

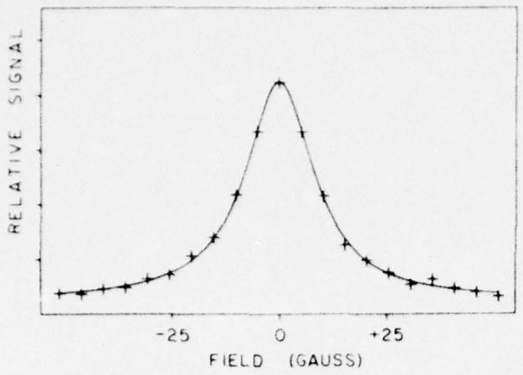

FIG. 2. Yb II Hanle signal fit with Lorentzian. The solid line is the computer fit.

in which the signal due to fluorescence reduces to a Lorentzian,

$$S = [1 + (2g\mu H\tau/\hbar)^2]^{-1}. \quad (1)$$

Here g is the Landé g factor, μ the Bohr magneton, H the field in gauss, τ the lifetime in seconds, and $\hbar$ Planck's constant reduced.

The decay constant obtained from this curve is then related to the radiative lifetime by

$$\Gamma^{(L)} = \Gamma - \sum_i \alpha_i^{(L)} x_i \Gamma_i + \gamma_L, \quad (2)$$

with the parameters as given by Saloman and Happer.[12] The radiative lifetime τ_0 is just $1/\Gamma$. In the limit of low Yb density which characterizes our work, x_i, the reabsorption probability, reduces to $K_i N$ and the expression becomes[13]

$$\frac{1}{\tau_{\text{eff}}} = \frac{1}{\tau_0} - \frac{1}{\tau_0} \sum_i \frac{\tau_0}{\tau_i} \alpha_i K_i N + n\sigma\bar{V}. \quad (3)$$

The first term on the right-hand side is the radiative lifetime, the middle term is due to radiation trapping, and the last term accounts for collisional depolarization. The coefficients α_i and K_i depend on the states involved. The sum is over i branches, with τ_0/τ_i the branching ratio for the ith branch. N is the Yb density. In the last term n is the helium density, σ the alignment depolarization cross section, and $\bar{V}$ the average relative collisional velocity.

All data were taken by accumulating signal vs magnetic field with a Fabri-Tek 1060 signal averager. The resulting curve was plotted on an x-y recorder. All plots were subsequently digitized by a Tektronix Graphics Tablet and the full width at half-height was extracted by a nonlinear least-squares fit to a Lorentzian. A typical fit is shown in Fig. 2. In order to obtain the radiative lifetime a double extrapolation was used. For each helium pressure a set of line widths vs Yb density was extrapolated to zero Yb density by a least-squares fit to a straight line, thus leaving the data independent of Yb density. A typical extrapolation of the linewidth to zero Yb density is shown in Fig. 3. The relative density is obtained from the intensity of the resonance fluorescence. A number of width measurements were taken at each Yb density to reduce random error. The peak-to-peak scatter among the widths at each density was seldom over 4% and on the average was under 2%. Finally, the width vs helium pressure data was plotted and least-squares fitted by a straight line. From the intercept and slope of this line the radiative lifetime and alignment depolarization cross section were deduced. The plot of width vs helium pressure for the $4f^{14}6s6p\,^3P_1$ level is shown in Fig. 4 as an example.

The next consideration was that of hyperfine effects. Ytterbium has a 30% natural abundance of odd isotope, with 14% spin-$\frac{1}{2}$ and 16% spin-$\frac{5}{2}$. Even with a 30% abundance one would expect the effect on lifetime measurements to be a few per-

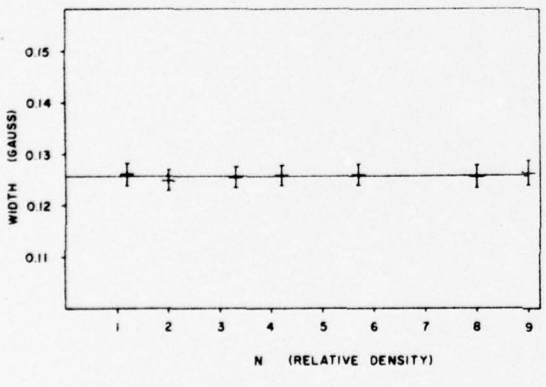

FIG. 3. Linewidth vs Yb density for the $4f^{14}6s6p\,^3P_1^o$ level. The horizontal scale is in units of scattered fluorescent intensity, which is linearly related to the Yb density.

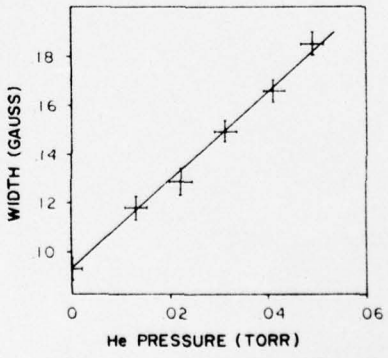

FIG. 4. Width vs helium pressure plot for the $4f^{14}6s6p\,^3P_1^o$ levels.

TABLE I. Experimental results.

Line (Å)	Term	Configuration	g_J	Present data σ (10^{-15} cm^2)	Present data τ (nsec)	Other data τ (nsec)
				Yb I		
5556	$^3P_1^o$	$4f^{14}6s6p$	1.48	5.0(1.0)	820(20)	827(40) [a] 760(80) [b] 850(80) [c] 980(70) [d]
3988	$^1P_1^o$	$4f^{14}6s6p$	1.035	5.9(1.0)	5.12(0.12)	5.5(0.25) [a] 12 [f] 5.63(0.25) [e] 6.4(0.2) [d]
3464	$(3\frac{1}{2},3\frac{1}{2})_1^o$	$4f^{13}5d6s^2$	1.26	5.9(1.2)	14.4(0.5)	17 [b] 14.3(0.9) [e] 18.3 [d]
2672	$(?)_1^o$	?	1.02	17.9(2.0)	77.4(6.0)	57.3(4) [e] 93 [d]
2464	$^1P_1^o$	$4f^{14}6s7p$	1.01	28.2(3.0)	9.3(0.6)	10.4(1.5) [e] 12.4 [d]
2272	$^1P_1^o$	$4f^{14}6s8p$	1.00	51.6(4.0)	39.1(3.5)	
				Yb II		
3290	$^2P_{3/2}^o$	$4f^{14}6p$	1.333	7.2(2.5)	5.8(0.6)	7.3(0.6) [c]

[a] M. Baumann and G. Wandel, Ref. 5.
[b] B. Budick and J. Snir, Ref. 9.
[c] M. L. Burshtein *et al.*, Ref. 8.
[d] V. A. Komarovskii and N. P. Penkin, Ref. 6.
[e] W. Lange *et al.*, Ref. 7.
[f] B. Budick and J. Snir, Ref. 10.

cent at most.[14] A careful analysis of the hyperfine structure supports this claim. Assuming a flat lamp profile, it was found for our method of analyzing the Hanle curves the lifetimes could be 3% and 5% longer for neutrals and ions, respectively, than uncorrected results would suggest. The details of these calculations are given in the Appendix.

A unique complication arises with the ion Hanle signal. The Penning reaction which produces our ground-state ion density heavily populates the $4f^{14}6p$ level. The resulting radiation at 3290 Å is much greater than the Hanle signal and obscures the direct observation on the oscilloscope. Since the ions interact with the applied magnetic field, the ion density is a slowly varying function of field. In order to unscramble the Hanle signal a procedure similar to that of Smith and Gallagher[15] was employed, in which two sets of curves are taken. One set is taken with the polarizer parallel to the field and gives only the ion dependence on magnetic field. The other is taken with the polarizer perpendicular to the field and gives a composite of the Hanle signal with the ion-density field dependence. The result of this correction fitted to a Lorentzian is shown in Fig. 2.

RESULTS

Our data represent the first lifetime measurements made on ytterbium in a flowing system. We were able to extend the number of level lifetimes measured (the $4f^{14}6s8p$ radiating at 2272 Å) and to improve upon the accuracy of existing measurements. As a by-product of lifetime measurements in a flowing system we also obtained the first alignment depolarization cross sections for ytterbium with helium.

The experimental results are presented in Table I. Lifetimes are compared to those measured by other authors. It should be noted that the lifetimes of Komarovskii and Penkin[6] are not direct measurements but are calculated from oscillator strengths obtained by anomalous dispersion and total absorption. These measurements average some 20% longer than ours. Once this 20% adjustment is made the agreement is excellent, implying a systematic error in one technique or the other. The large value obtained for the $6s6p\,^1P_1^o$

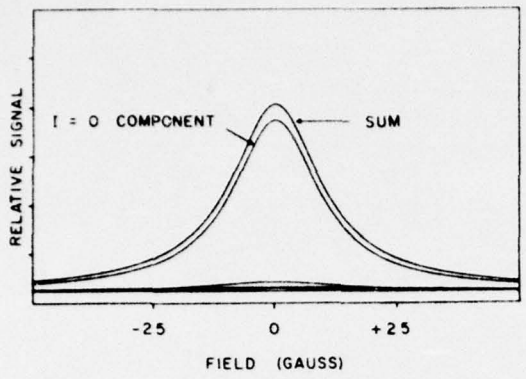

FIG. 5. Components of the Hanle signal for $J = 1$ Yb I levels.

lifetime by other workers using the Hanle technique can probably be explained by coherence narrowing, in view of this level's large oscillator strength. Our excellent agreement with other Hanle effect and delayed coincidence measurements of the $6s6p\,^3P_1$ level lifetime, which has an oscillator strength 100 times smaller than the singlet level, supports this claim. This gives us confidence in our lifetime measurement of the $6s8p\,^1P_1^o$ level reported here for the first time and in the lifetime of the $6p\,^2P_{3/2}^o$ ion level.

The lifetimes given in Table I do not contain a correction for hyperfine effects. As discussed in the Appendix, these could result in as much as a 3% increase in neutral lifetime and a 5% increase in the $6p$ ion level lifetime. If this correction is included, our value for the Yb II $^2P_{3/2}^o$ level becomes 6.09 ± 0.6 nsec, which agrees with the value of Burshtein *et al.* at the limits of experimental error. We chose not to incorporate the hyperfine effect into the lifetime because of our lack of knowledge of the lamp profile, but rather state it as an added uncertainty.

Alignment depolarization cross sections are presented without comment save the qualitative observation that for higher nl states σ is larger. No attempt was made to bring the uncertainties for the cross sections in line with those of the lifetimes. The larger experimental errors are due mostly to lack of data over a wide enough pressure range for some of the small width/Torr slopes encountered when plotting width vs helium pressure.

APPENDIX

Using the standard vector coupling coefficients of Condon and Shortley[16] and assuming a broadband "white light"[17] source we obtained the following expression for the signal from the $J = 0$ to $J = 1$ transitions in Yb with nuclear spins $I = 0$, $\frac{1}{2}$, and $\frac{5}{2}$:

$$S = 1 - 0.808(\cos^2\alpha \sin^2\alpha' + \cos^2\alpha' \sin^2\alpha) + 0.808 \cos^2\alpha \cos^2\alpha' - \sin^2\alpha \sin^2\alpha' \left(\frac{0.7}{1+x^2} + \frac{0.06}{1+(0.667x)^2} + \frac{0.001}{1+(0.4x)^2} + \frac{0.026}{1+(0.267x)^2} + \frac{0.021}{1+(1.2x)^2} \right), \quad (4)$$

with

$$x = 2g_J \mu H \tau / \hbar.$$

Here α and α' are the angles the polarization vector makes with the magnetic field direction for incident and reflected beams, respectively. In this experiment we used a polarizer on the detector for all wavelengths above 2672 Å and no polarizers for 2672 Å and below. Upon analyzing the broadening produced with and without the polarizer we found the difference to be completely negligible.

To determine the extent of broadening, the sum of the Lorentzian was compared to a simple Lorentzian ($I = 0$ case) by the least-squares-fit program. Also, each Lorentzian component, together with the sum, was plotted and is shown in Fig. 5. It becomes apparent that the very broad components approximate a constant background and thus have little effect on the width of the sum except far into the wings. Using the least-squares fit we found approximately to 2–3% increase in the full width at half-height over the $I = 0$ case, which implies that the lifetime is 2–3% longer than the uncorrected results would suggest.

An identical procedure was followed for the ion. The signal as a function of polarization angle was found to be

$$S = 1 - 0.470\,(\cos^2\alpha \sin^2\alpha' + \cos^2\alpha' \sin^2\alpha) + 0.470 \cos^2\alpha \cos^2\alpha' - \sin^2\alpha \sin^{-2}\alpha' \left(\frac{0.42}{1+x^2} + \frac{0.019}{1+(1.25)^2} + \frac{0.043}{1+x^2} + \frac{0.0003}{1+x^2} + \frac{0.005}{1+(0.083x)^2} + \frac{0.001}{1+(0.292x)^2} + \frac{0.017}{1+(0.375x)^2} \right). \quad (5)$$

The effect on measured lifetime in this case is 3–5%, again depending upon how far into the wings the least-squares fit was made.

*Research supported by Office of Naval Research under Contract No. ONR-N00014-69-A-0141-0004.

[1]W. Hanle, Z. Phys. 30, 93 (1924).
[2]J. Tech, J. Res. Natl. Bur. Stand (U.S.) (to be published).
[3]W. F. Meggers and B. F. Scribner, J. Res. Natl. Bur. Stand. (U.S.) 19, 651 (1937).
[4]W. F. Meggers and C. H. Corliss, J. Res. Natl. Bur. Stand. (U.S.) A70, 63 (1966).
[5]M. Baumann and G. Wandel, Phys. Lett. 22, 283 (1966).
[6]V. A. Komarovskii and N. P. Penkin, Opt. Spektrosk. 26, 882 (1969) [Opt. Spectrosc. 26, 483 (1969)].
[7]W. Lange, J. Luther, and A. Steudel, Summaries of the Second European Group on Atomic Spectroscopy Conference, Hanover, 1970 (unpublished).
[8]M. L. Burshtein, Ya. F. Verolainen, V. A. Komarovskii, A. L. Osherovich, and N. P. Penkin, Opt. Spektrosk. 37, 617 (1974) [Opt. Spectrosc. 37, 351 (1974)].
[9]B. Budick and J. Snir, Phys. Rev. A 1, 545 (1970).
[10]B. Budick and J. Snir, Bull. Am. Phys. Soc. 12, 186 (1967).
[11]F. D. Colgrove and P. A. Franken, Phys. Rev. 119, 680 (1960).
[12]W. Happer and E. B. Saloman, Phys. Rev. 160, 23 (1967).
[13]W. W. Smith and A. Gallagher, Phys. Rev. 145, 26 (1966).
[14]See L. G. Williams and D. R. Crosley, Phys. Rev. A 9, 622 (1974); see also A. Gallagher, Phys. Rev. 157, 24 (1966), for a discussion of hyperfine effects.
[15]W. W. Smith and A. Gallagher, Phys. Rev. 145, 26 (1966).
[16]E. U. Condon and G. H. Shortley, *The Theory of Atomic Spectra* (Cambridge U. P., London, 1970), Chap. 3.
[17]One might expect our "white light" source to be a good approximation. The lamp pressure was on the order of 50 Torr with a current of 3 A. Thus Stark and pressure broadening could be expected to contribute significantly to the emission-line width.

Accepted for publication, Rev. Sci. Inst., Dec. 1976.

Intense flowing hollow cathode lamp*

F. H. K. Rambow and L. D. Schearer

Department of Physics, University of Missouri–Rolla, Rolla, Missouri 65401

(Received 9 April 1976; in final form, 30 August 1976)

An inexpensive, simple, and versatile hollow cathode lamp has been developed which produces intense ion resonance radiation of about 1 mW into $4\pi/25$ sr. The lamp employs flowing helium gas to sustain the discharge. The construction permits a variety of cathode seed materials to be easily interchanged. The same lamp has been used as a source of ion resonance radiation for Ca, Ba, Zn, Mg, Sr, Yb, and Eu.

We have succeeded in developing a flowing hollow cathode lamp with which we have measured radiative lifetimes of some Group II and rare earth ion levels.[1,2] The lamp is very simple and inexpensive to build. Since it operates on dc there are no problems of rf shielding. With reasonable care in construction and operation it is practically indestructible. Unlike sealed hollow cathode lamps the same lamp can be used for many elements and can be readily disassembled for cleaning and recharging. Welding grade helium is used as the flowing buffer gas because it is readily available and reasonable inexpensive. The use of flowing helium gas inhibits the condensation of material on the lamp windows and circumvents the necessity for high vacuum techniques in the preparation of the lamp.

A drawing of the lamp is shown in Fig. 1. The lamp is both air and water cooled for stability and long life. The anode is machined from a 3.81-cm brass cylinder. Water cooling is provided by a 4.8-mm-diam copper tube soldered around the anode. The inlet He stream flows across the quartz window on the front of the anode to prevent fogging by metal vapor deposits. The anode is supported by the outer jacket, a 2.54-cm-diam Pyrex tube 12.7 cm long. This tube is cooled by a stream of air. The window and Pyrex tube are attached to the anode by Dow Corning silicon rubber compound. The cathode is machined from a 9.8-mm rod of boron nitride and lined with 0.1-mm tantalum foil. It is supported by a stainless steel welding rod insulated by a small diameter Pyrex tube. The welding rod is attached to a 6.35-mm brass rod that extends out through an Ultra-Torr[3] fitting so that the anode–cathode spacing can be adjusted while the lamp is in operation. The entire cathode assembly is mounted to the glass jacket by an O-ring connector similar to the Ultra-Torr commercial fittings. This allows the cathode to be pulled out easily for recharging.

The lamp normally operates at 3 A with a helium pressure in the range 1–50 Torr. A flow rate on the order of 1×10^{5} atm cm^{3} min^{-1} is maintained. The power into a solid angle of $4\pi/25$ sr from the 4078 Å sr line was found to be 1×10^{-3} W or about 2×10^{15} quanta sec^{-1}. Compared to prevous lamp designs the flowing hollow cathode lamp described here provides excellent versatility and ease of construction without sacrificing intensity.[4] The lamp described by Weber[5] has greater intensity (10^{16} quanta sec^{-1} into $4\pi/25$ sr; however, the current required to obtain this output is 30–40 A.

Our design, in addition to high intensity, allows a wide range of materials to be used in the cathode, and furthermore this material can be changed in minutes. The lamp can be opened to air, the cathode assembly pulled out, cleaned in nitric acid, reinserted, and run to bake out water vapor, pulled out and charged with a new material, and be running, all within five minutes. We have used this source with Ca, Sr, Mg, Ba, Zn, Cd, Yb, and Eu.

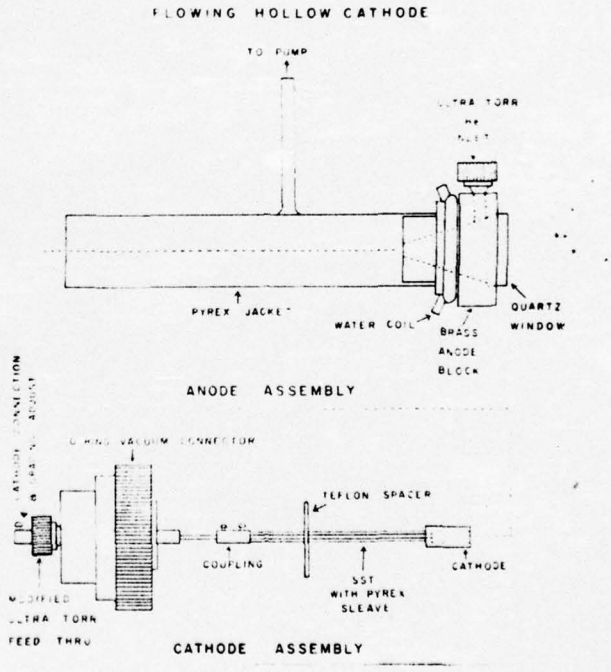

FIG. 1. Flowing hollow cathode lamp. Air is blown over the Pyrex jacket near the discharge region.

* [1] F. H. K. Rambow and L. D. Schearer, Bull. Am. Phys. Soc. **20**, 1448 (1975).
[2] F. H. K. Rambow and L. D. Schearer, Phys. Rev. A **14**, 738 (1976).
[3] Ultra Torr is a trde name of Cajon Co., Cleveland, OH.
[4] B. Budick, R. Novick, and A. Lurio, Appl. Opt. **4**, 229 (1965).
[5] E. W. Webber, Z. Phys. **256**, 1 (1972).

Proceedings 5th International Conference on Atomic Physics, Berkeley, CA, July 26-30, 1976.

THE VIOLATION OF THE FRANCK-CONDON PRINCIPLE IN PENNING IONIZATION

W. F. Parks

University of Missouri - Rolla, Rolla, Mo. 65401 USA

It has been generally assumed that Penning ionization can be described as a Franck-Condon process. It is shown that the electronic transition amplitudes encountered in Penning ionization are not in general slowly varying functions of the interatomic distance in comparison to the variation of the interatomic wave functions. The necessary conditions for application of the Franck-Condon are therefore not satisfied and the assumption is in error. An immediate result is that the rather simple relationship between the energy distribution of the ejected electrons and the interatomic potential curves developed in the semiclassical theory will not hold. In that theory the possible energies of the ejected electrons depend on the structure of the interatomic potentials. In contrast when the assumption of the Franck-Condon principle is not made it is found that, with typical electronic transition amplitudes, the energy distribution will have an appreciable width even in the absence of potential variations.

As examples the electron energy distributions found[1,2] for the processes

$$He^M(^3S) + H \longrightarrow He + H^+ + e$$

and

$$He^M(^3S) + A \longrightarrow He + A^+ + e$$

are discussed.

*Work supported in part by the U. S. Office of Naval Research

[1] H. Hotop, E. Illenberger, H. Morgner, and A. Niehaus, Chem. Phys. Letters 10, 493 (1971)

[2] H. Hotop, A. Niehaus, and A. L. Schmeltekopf, Z. Phys. 229, 1 (1969).

Accepted for publication, J. Chem. Phys., Dec. 1976.

RADIATIVE LIFETIME OF THE $A^2\Delta$ STATE OF CH*

James Carozza and Richard Anderson

Department of Physics
University of Missouri-Rolla, Missouri

ABSTRACT

The lifetime of various rotational levels of the v' = 0 and 1 vibrational states of the $A^2\Delta$ state of CH are reported. The lifetimes for the various levels were nearly constant with the rotational quantum number N'. For the v' = 0 level it was 508 $\pm$ 25 ns and for the v' = 1 level, it was 514 $\pm$ 33 ns. The band head lifetime was 500 ns and these lifetimes are very close to the band head lifetime.

The present investigation was begun because of the unusual results reported by Anderson, et. al.[1] They reported irregular variations of lifetime over the band corresponding to the $A^2\Delta$ - $X^2\pi$ transition in CH. They made measurements at various positions in the band with a low resolution monochromator and could not resolve individual rotational transitions. They excited the CH radical with a pulsed r-f discharge which was terminated in 15 ns, but the decay curves were recorded on a boxcar integrator and X-Y recorder. As a result, they could not measure weak CH emissions. Since there is a many-line H_2 spectrum in this region, the possibility of overlap of CH and H_2 lines could not be ruled out.

In the present study the same pulsed r-f discharge was employed, but the spectral lines were resolved on 3/4 m Spex monochromator with a 0.1A resolution and weaker signals could be observed since the delayed coincidence detection technique was used. Now the rotational lines of the $A^2\Delta$ - $X^2\pi$ transition were resolved from the heavily quenched H_2 lines. A similar effect was noted in our measurements of the lifetime of the rotational levels of the $B^2\Sigma^-$ state[2]. This overlap of the CH and H_2 spectra at low CH_4 pressures made it difficult to measure the CH lifetimes accurately at very low pressures.

Erman[3] has measured the lifetime of rotational levels of the vibrational v' = 0 and 1 levels for the $A^2\Delta$ state by the high frequency deflection method in which an electron beam is rapidly terminated by high frequency deflection of it past a slit. He could resolve Λ doubling components. The lifetimes for both Λ doubling components of the rotational states N' = 6 to 23 for the vibrational level v' = 0 were nearly constant and both had the same value of 534 + 5 ns. However, a different behavior was observed for the lifetime of the rotational levels of the v' = 1

state. In this case the lifetime for both Λ doubling components decreased continuously for N' > 11 between 11 and 16. The lifetime of the "d" component reached an almost constant value of 365 ns for N' $\geq$ 16, while the "c" component passed through a minimum of 354 ns at N' = 18 and increased again to 368 ns at N' = 20. The N' = 11 level coincides with the dissociation limit of the $X^2\pi$ ground state and he interpreted this behavior as an unobserved predissociation of the CH A state by the overlap of the vibrational wavefunctions of the $A^2\Delta$ state with the continuum wavefunction of the $X^2\pi$ ground state. A spin-orbit and rotational-electronic coupling leads to a predissociation of this type.[4]

In our study the Λ doubling components could not be resolved. We observed a nearly constant lifetime of the rotational levels of the v' = 0 state for N' = 6 to 20. This result agreed with those observed by Erman, except our constant value was approximately 508 $\pm$ 25 ns. This was very close to the band head lifetime of the system which is 500 ns. From our limited measurements of the rotational levels for the v' = 1 vibrational state there may not be a drop in lifetime. From our limited measurements the lifetime was 514 $\pm$ 33 ns which is similar to the value obtained for the rotational states of the v' = 0 levels. The data are displayed in Figure 1.

The difference between our data and those of Erman[3] may be caused by the erroneous removal of the lifetime of the H_2 lines from the data which will tend to produce a complex decay. The H_2 molecular emission has a zero pressure lifetime near 100 ns. Further, any nitrogen impurity could cause an error in lifetime measurements. The first negative system of N_2^+ has an intense, extended band system starting at 4278A and extending to 4130A. The N_2^+ first negative zero pressure lifetime is 65 ns. This

experiment should be repeated by some other investigators with a different technique, for its results may explain the formation of CH in interstellar space. If a predissociation of the v' = 1 level of the $A^2\Delta$ state by the $X^2\pi$ state is possible, this is a possible inverse mechanism for the formation of the CH molecule observed in interstellar space.

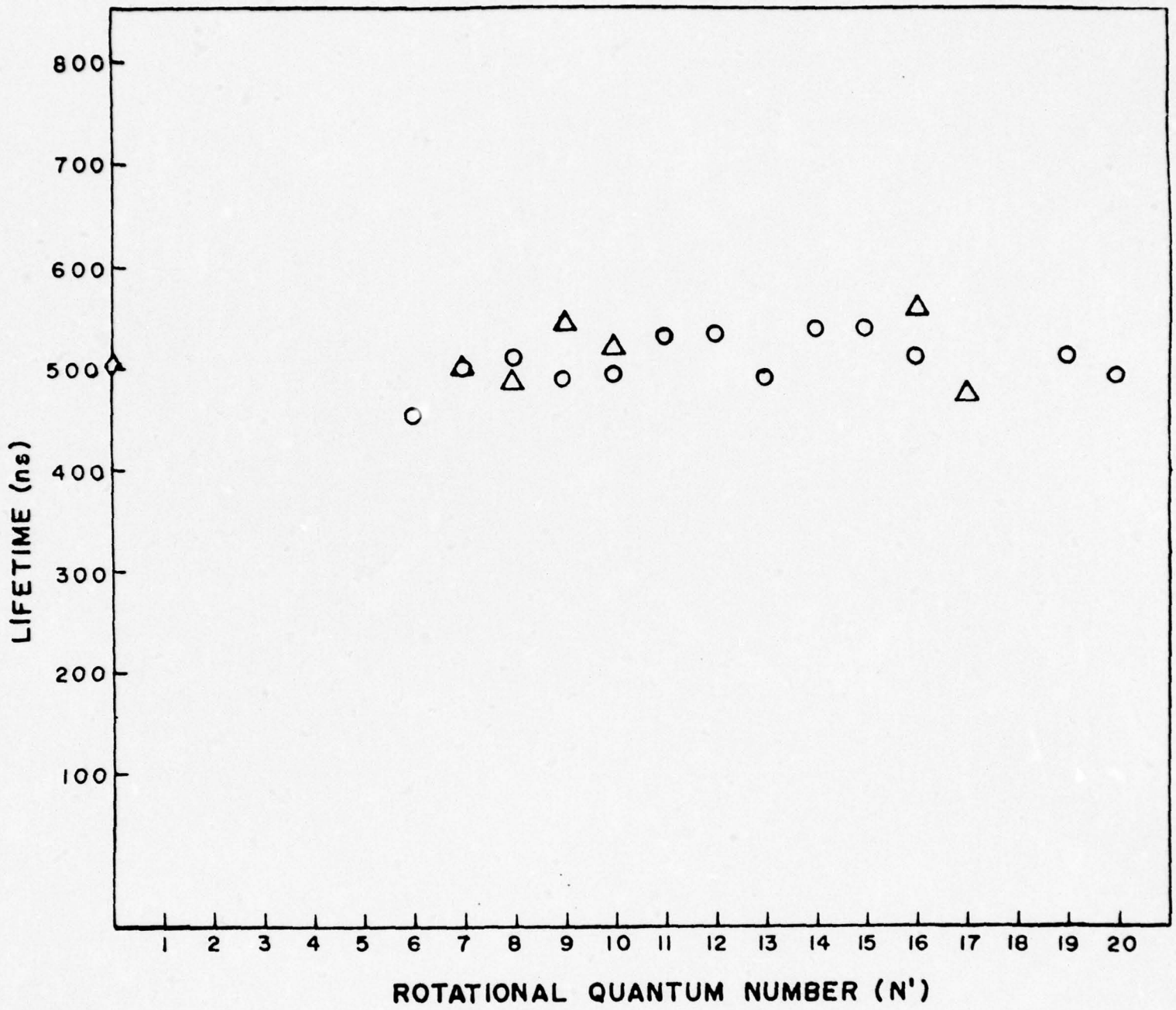
800
700
600
500
400
300
200
100
LIFETIME (ns)
1 2 3 4 5 6 7 8 9 10 11 12 13 14 15 16 17 18 19 20
ROTATIONAL QUANTUM NUMBER (N')

Caption

Figure 1. The lifetime of rotational levels of the $A^2\Delta$ state. o corresponds to v' = 0 levels, Δ corresponds to v' = 1 levels, and ◇ corresponds to the band head lifetime.

References

This research was supported under ONR grant N00014-75-C-0477.

1. R. Anderson, R. Sutherland, and D. Wilcox, "Radiative Properties of CH and CH^+ Molecular States," Nuclear Instruments and Methods, 110, 167 (1973).

2. R. A. Anderson, J. Peacher, and D. M. Wilcox, "Radiative Lifetime of the $B^2\Sigma^-$ State of CH," J. Chem. Phys., 63, 5287 (1975).

3. P. Erman, "Applications of High Resolution Measurements of Optical Lifetimes," Proc. of the 4th Int. Beam Foil Conf., Gatlinburg, Tenn., U.S.A., Sept. 15-19, 1975.

4. I. Kovacs, "Rotational Structure in the Spectra of Diatomic Molecules," American Elsevier Publishing Co., Inc., New York (1969).

A High-Power Pulsed Xenon Ion Laser as a Pump Source for a Tunable Dye Laser

LAIRD D. SCHEARER

Abstract—**An inexpensive pulsed xenon ion laser with peak power outputs up to 4 kW has been constructed and used as a pump source for a tunable rhodamine 6G dye laser with a 0.25-Å bandpass in the yellow-red range of the spectrum. The dye laser is tunable from 5465 to 6300 Å. Over 50 W are obtained at the peak of the tuning range.**

I. Introduction

THERE has been considerable recent interest in the pulsed xenon ion laser [1]-[4]. The interest stems primarily from the simplicity of a high-gain laser system which is capable of relatively high peak power emission in the blue-green region of the spectrum accompanied by relatively long pulsewidths. We have investigated the properties of a high-power pulsed xenon ion laser and its use as a pump source for a tunable dye laser. Peak pulse powers of 4 kW and pulse durations up to 1 μs have been obtained in a 120-cm × 4-mm xenon discharge at pressures between 5 and 30 m · torr. The high peak power available in the xenon laser has enabled us to use it as a pump source for a rhodamine 6G dye laser which is tunable from 5465 to 6300 Å with a 0.25-Å bandwidth. At the peak of the dye laser output, ~ 5750 Å, we obtain over 50 W of peak power with 500-ns pulsewidths.

In the sections following we describe the operating characteristics of our pulsed xenon laser and its use as a pump source in the design and construction of the tunable dye laser system.

II. Xenon Ion Laser

Data obtained in earlier work on this type laser system are summarized in Table I along with the results of our work. It is important to note that, based on the volume of the excited gas, the work reported here represents a substantial improvement in both the peak pulse power and pulse duration obtained. In particular, we compare the results of our work with that of Hänsch *et al.* [3]. It was the report of their work on the xenon laser and dye laser that provided the initial motivation for the work we report here. The particular aspect of the Hänsch *et al.* work which attracted our attention was the low construction cost and simplicity of design of the xenon laser and the dye laser system.

The only work which reports a higher peak power than that reported here is that of Gundersen and Harper [4] who obtained approximately 80-kW peak pulse power. Their laser tube, however, was over 10 ft in length with a bore area approximately 20 times greater than the one we used.

TABLE I
SUMMARY OF RECENT WORK ON PULSED XENON ION LASERS

Hänsch *et al.* [3]	120	4.0	100	0.1
Gundersen and Harper [4]	100	17.0	80,000	0.11 - 0.2
This work	120	4.0	4,000	0.1 - 1.5

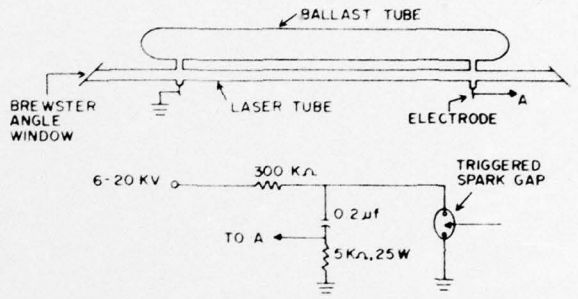

Fig. 1. Pulsed xenon ion laser and electrical discharge circuit.

The active length of the discharge tube was 120 cm with a bore diameter of 4 mm. The laser tube length was supplemented by an additional 25 cm at each end between the internal electrodes and the windows which terminated the laser tube. The electrodes are high-current indium cathodes constructed by melting pure indium metal around the tungsten electrodes [5]. The additional spacing between the electrodes and Brewster windows was provided to reduce the possibility of window contamination by sputtering of the metal at the electrodes. The laser tube also included a ballast tube as shown in Fig. 1.

We utilized a number of electrical circuits for the pulsed excitation of the laser discharge tube. The first method and probably the simplest we utilized was that described by Hänsch *et al.* in their report on the xenon laser [3]. The power supply consisted of a 15-kV 60-mA high-voltage transformer of the type used to excite neon signs and a bank of twenty-two 500-pF capacitors connected across the transformer terminals and laser electrodes. In this condition the laser tube discharged at a 120-Hz rate, i.e., on each half-cycle.

With an 80-percent output reflector in place we obtained

Manuscript received June 16, 1975. This work was supported in part by the Air Force Office of Scientific Research under Contract 2672, and in part by the Office of Naval Research under Contract N00014-75C-0477.

The author is with the Department of Physics, University of Missouri at Rolla, Rolla, Mo. 65401.

results identical with those reported by Hansch *et al.* [3]. There were eight visible lines observed in laser emission ranging from the violet at 4306 Å to the orange at 5956 Å. The maximum peak power output obtained was 300 W with laser pulsewidths up to 350 ns.

With the circuit described previously the pulse repetition rate was erratic with many skipped pulses. We had additional difficulty with periodic failure of the doorknob capacitors. As a result of these difficulties we abandoned this excitation method and constructed a spark-gap-triggered discharge. The important features of the spark gap are its exceptionally low inductance, its capacity for holding off high voltages, and when it does break down, its capacity of transferring large quantities of electrical charge. Our triggered spark gap has properties similar to those of commercial manufacture.

The capacitive discharge circuit is shown as part of Fig. 1. When the properties of the laser system were evaluated with this circuit we obtained a substantial increase in both peak power and laser pulse duration.

The peak pulse power obtained and the pulsewidth as a function of the charging voltage on a 0.2-μF capacitor are shown in Fig. 2. These data were obtained when the laser pressure was optimized for maximum power. Table II summarizes typical peak powers obtained for seven of the eight observed transitions.

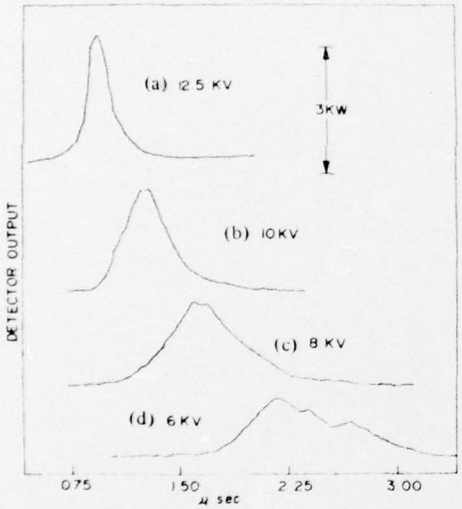

Fig. 2. Laser pulse shapes obtained at various charging voltages for a 0.2-μF capacitor. The curves were obtained with a high-speed silicon photodiode and a PAR boxcar integrator. The scale shown on the horizontal axes represents time delays after a trigger pulse is applied to the spark gap.

TABLE II
PEAK POWER ON OBSERVED LASER LINES

Wavelength (Å)	Peak power (watts)
5956	110
5395	480
5353	800
5260	680
5190	250
4954	800
4306	50

This laser system was capable of repetition rates from single shot up to 30 Hz. The upper limit is determined by the present capacity of our power supply. From the energy-per-pulse measurement and the repetition rate one can obtain the *average* laser power output. The highest average power we obtained was approximately 20 mW.

The data shown were obtained with an 80-percent broadband reflecting output mirror. In an effort to determine the optimum output coupling we repeated the power measurements for output mirror reflectivities of 98, 50, and 20 percent. At 98 percent, the power output was reduced by a factor of 2. At 20 percent the output power was down an order of magnitude, while with the 50-percent mirror similar results were obtained. We thus conclude that the mirror reflectivity required for optimum power output lies between 50 and 80 percent.

The availability of substantial laser output power even with mirrors which transmit 80 percent of the incident optical energy is an indication of the relatively large gain of several of the laser transitions. This in turn suggests that relatively lossy elements can be inserted in the optical cavity while still maintaining laser action. As a next step in this work the addition of a nonlinear crystal in the optical cavity is planned to attempt intracavity frequency doubling of the Xe ion laser emission.

III. The Tunable Dye Laser Cavity

Several dye laser cavitites have been developed in the past for use in CW dye laser applications. In these systems one needs a cavity design which provides an intracavity focus to meet the pumping requirements. In CW systems pump power is at a premium and the pump beam is generally focused to a small spot to provide a high energy density within the dye. One also desires a long cavity length as well, for tuning purposes.

Cavity configurations which satisfy these requirements are resonators with an internal lens or the equivalent three-mirror cavity [6].

Hänsch *et al.* constructed a three-mirror resonator and pumped the dye with the output of their pulsed xenon ion laser. With rhodamine 6G dye they obtained 12 W of peak power at 5700 Å. The resolution of the dye laser emission they reported as <100 Å. However, they did not include a frequency-selective element inside the dye laser cavity. Consequently, the dye laser output was not tunable and their laser output had poor resolution.

The three-mirror resonator of [6] was modified slightly by replacing the flat mirror (1) by a 1200-l/mm grating in Littrow mount as shown in Fig. 3. Mirrors 1 and 2 are highly reflective over a broad band and have radii of curvature of 5 and 10 cm, respectively. When the mirrors are separated by 10 cm there is a tightly focused spot at the center of the 2 mirrors. At this point a cell of thickness 1 mm containing a 10^{-3} M solution of rhodamine 6G dye in ethanol is inserted at Brewster's angle. The dye is contained in a sealed cell. It

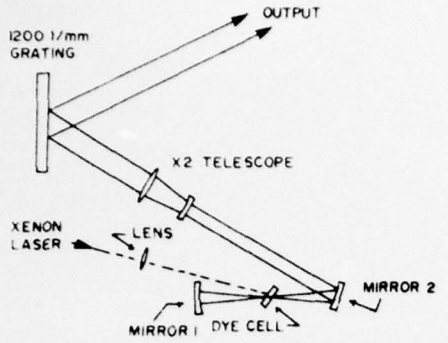

Fig. 3. The astigmatic dye cavity. A 1200-l/mm grating is used as the output reflector.

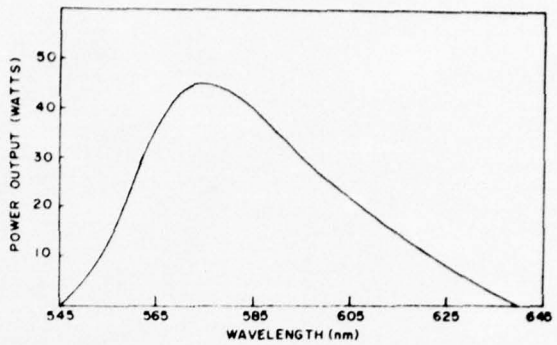

Fig. 4. Power tuning curve for rhodamine 6G. Bandwidth is less than 0.25 Å over entire range. Pulsewidth is 350 ns. Pump power is approximately 1.6 kW.

was found unnecessary to flow the dye. The grating is located 25 cm from mirror 2. A two-power telescope is used inside the cavity as shown to expand the beam on the grating.

The xenon ion laser light is focused on the dye cell by a 20-cm fL spherical lens as shown. When properly adjusted the dye system lases with no difficulty. The dye output is taken from the zero-order diffraction from the grating which was blazed for 5000 Å. No system degradation over many days was observed by using a sealed dye cell containing 0.1 ml at repetition rates to 30 Hz.

With the dye laser system described in the preceding section pumped by our xenon ion laser we were able to obtain substantially higher peak power outputs from the dye laser than that reported by Hansch *et al.* In addition, the presence of the grating permits tuning of the dye laser output and results in a much higher resolution of the laser emission.

Our tuning width with rhodamine 6G ranged from approximately 5465 to 6300 Å, with a bandwidth of less than 0.25 Å. The peak output power at the center of the tuning range was 50 W. The dye laser pulsewidth was slightly shorter (~20 percent) than the xenon pump pulse. The power tuning range we obtained for rhodamine 6G is shown in Fig. 4. The dye laser gain pumped by the xenon laser is sufficiently great that the system lases even when a clear quartz plate is used as the output reflector.

This is the first reported instance of a tunable dye pumped by a repetitively pulsed xenon ion laser. Without the telescope, the dye laser bandwidth was about 2 Å with a peak power output of 100 W at the center of the tuning range.

Rhodamine B dye was used also; contrary to expectations it did not provide operation further into the red than rhodamine 6G. This may be more a property of the dye mirrors and grating used which were standard commercial reflectors for rhodamine 6G than any inherent difficulties with the pumping source.

The attractive features of this xenon pumped dye laser are the relatively high repetition rates and the relatively long pulsewidths available in a simple, inexpensive system. The 0.25-Å bandpass obtainable with the grating telescope combination should make this a valuable tool in atomic spectroscopy. We also note that a considerable improvement in the efficiency of the system and the bandwidth should be possible by using coated optics in the telescope and, in general, by upgrading the quality of the components.

Acknowledgment

The author wishes to thank W. Hoffman and S. Price for assistance in the design and construction of the lasers.

References

[1] V. Hoffman and P. Toschek, "New laser emission from ionized xenon," *IEEE J. Quantum Electron.* (Notes and Lines), vol. QE-6, p. 757, Nov. 1970.

[2] W. W. Simmons and R. S. Witte, "High-power pulsed xenon ion lasers," *IEEE J. Quantum Electron.*, vol. QE-6, pp. 466-469, July 1970.

[3] T. W. Hänsch, A. L. Schawlow, and P. Toschek, "Simple dye laser repetitively pumped by a xenon ion laser," *IEEE J. Quantum Electron.* (Corresp.), vol. QE-9, pp. 553-554, May 1973.

[4] M. Gundersen and C. D. Harper, "A high-power pulsed xenon ion laser," *IEEE J. Quantum Electron.* (Notes and Lines), vol. QE-10, p. 1160, Dec. 1973.

[5] W. W. Simmons and R. S. Witte, "New cold cathode for pulsed ion laser," *IEEE J. Quantum Electron.* (Corresp.), vol. QE-6, pp. 648-649, Oct. 1970.

[6] H. W. Kogelnick, E. P. Ippen, A. Dienes, and C. V. Shank, "Astigmatically compensated cavities for CW dye laser," *IEEE J. Quantum Electron.*, vol. QE-8, pp. 373-379, Mar. 1972.

PHYSICAL REVIEW A VOLUME 14, NUMBER 5 NOVEMBER 1976

Radiative lifetimes of some group II ions by the Hanle effect in a fast-flowing helium afterglow*

F. H. K. Rambow and L. D. Schearer
Physics Department, University of Missouri-Rolla, Rolla, Missouri 65401
(Received 1 July 1976)

Radiative lifetimes of the first $^2P_{3/2}$ state of Mg II, Ca II, Zn II, Sr II, Cd II, and Ba II are reported as measured by the Hanle effect in a fast-flowing helium afterglow. They are, respectively, 3.65(0.12), 6.61(0.30), 2.4(0.3), 6.64(0.10), 2.86(0.25), 6.78(0.40) in units of 10^{-8} sec. The ions in the afterglow are created by Penning ionization of the neutral metal atoms, thus providing a steady-state, field-free region for observation. Comparisons are made with measurements by other methods, and discrepancies are discussed.

INTRODUCTION

Radiative lifetimes and depolarization cross sections are important parameters of excited states of ions. They serve not only as a test of existing theories but are also useful for astrophysical calculations and for understanding relaxation mechanisms in discharges and afterglows. We have measured radiative lifetimes of the first $^2P_{3/2}$ level of six group II ions by the Hanle[1] effect in a fast-flowing helium afterglow. These are the first measurements on group II ions reported in a flowing afterglow.

Until the Hanle measurements of Smith and Gallagher it was common to have uncertainties on the order of ±30% in the measurements of group II excited-ion lifetimes.[2,3] Some of this earlier work utilized the Hook method[4] and the arc method.[5] In the case of the Hook method, the large uncertainty was mostly due to the difficulty in measuring the ion density absolutely. The accuracy of the Hanle technique, on the other hand, depends only on knowing the relative densities, or working in the limit of very low densities at which collisional and radiation trapping effects vanish.

Gallagher and Smith reduced these large uncertainties to ±5% or less by the Hanle effect in a pulsed argon afterglow for several group II ions. A recent measurement of Kelly *et al.*[6] by the Hanle effect on the Sr II $^2P_{3/2}$ lifetime departed seriously from the value reported by Gallagher and Smith. Kelly reported measuring a very large depolarization cross section with the Sr neutral, and also obtained a lifetime some 15% shorter than Gallagher's value. Kelly's measurements were made by the Hanle effect in a cw discharge of Sr without a noble-gas buffer. This large difference in the Sr II lifetime, together with the lack of high-precision data on most group II ions (other than Gallagher's) led us to remeasure the radiative lifetimes of several group II ions in the $^2P_{3/2}$ state.

APPARATUS

The flowing afterglow is especially well suited for measuring lifetimes and alignment depolarization cross sections by the Hanle effect. It allows for rapid change and easy monitoring of system parameters, such as relative ion density and buffer-gas pressure. Thus, collisional depolarization and coherence narrowing can easily be controlled and their effects observed. Also the material under study can be quickly and easily changed so that lifetimes of many different species can be studied in the same apparatus over a short period of time. Another advantage is that, unlike a beam apparatus or a sealed cell, high-vacuum techniques are not necessary since flow rates are many orders of magnitude greater than outgassing rates.

Since the techniques and apparatus utilized here were reported in detail in a previous paper on Yb,[7] only a brief discussion of a few pertinent features appears here. The flow tube is evacuated by a 540 $ft^3 min^{-1}$ mechanical pump and a Roots blower. Flow velocities are on the order of 10^4 $cm\,sec^{-1}$ with background helium pressures in the range of 0.1–1 Torr. Of particular interest is the method of production of the ion ground-state density. A microwave cavity at the entrance to the flow tube is used to produce a discharge in helium. By the time the flow reaches the interaction region, the major constituents are helium metastables and helium neutrals. With a judicious setting of the discharge intensity, a helium metastable density on the order of 10^{11} cm^{-3} can be obtained in the interaction region with a background helium neutral density on the order of 10^{16} cm^{-3} and a helium ion density of about 10^{10} cm^{-3}. The reactant neutral is titrated into the interaction region by a furnace wound with coaxial heater wire. Penning ionization by the helium metastables (He^m) produces copious quantities of the reactant ions in steady state in a field-free region. Typical cross sections for this familiar reaction, $He^m + X \rightarrow He$

$+X^+ + e$, are greater than 10^{-15} cm^2.[8] Here X is the reactant atom. Ion densities as high as 10^{10} cm^{-3} are estimated by optical absorption. This technique for producing ions releases us from concerns over perturbations due to an ionizing electric field, and decreases necessary signal accumulation times over pulsed techniques. Another advantage of this configuration is the *in situ* magnetic field calibration it allows. The He^m atoms are optically pumped, and magnetic resonance is performed with the 10 830 Å light monitored in transmission, thus creating a helium magnetometer.

EXPERIMENTAL TECHNIQUE

Briefly, the Hanle effect is a well used zero-field level crossing technique, in which optical resonance radiation is used to coherently excite atoms in the presence of a magnetic field. The resulting fluorescence is plotted as a function of the magnetic field, and from this plot the lifetime can be obtained as a function of the g factor. Measurement methods were described in detail in Ref. 7. They will be only briefly reiterated here. The geometry and polarization used is such that the Hanle signal reduces to a Lorentzian, $(1+X^2)^{-1}$ where $x = 2g\mu H\tau/h$. Here g is the Lande g factor, μ the Bohr magneton, H the magnetic field, τ the lifetime, and h Plank's constant reduced.

A unique complication arises with the ion Hanle signal. Since the ions interact with the magnetic field, the ion density is a slowly varying smooth function of the magnetic field. Also, the Penning reaction heavily populates the $^2P_{3/2}$ ion level. The intensity from the resulting transition, $^2P_{3/2}-{}^2S_{1/2}$, obscures the direct observation of the Hanle signal on an oscilloscope, and shows the same ion-density field dependence. Field-dependent intensity variations of the ion emission in the absence of the optical resonance excitation were subtracted from the Hanle signals on alternate sweeps of the magnetic field. From this information, the ion field dependence was removed from the Hanle signal.

The corrected Hanle signal was then computer fitted to a Lorentzian by a nonlinear least-squares technique. A typical result of the corrected signal fit to a Lorentzian is shown in Fig. 1. An attempt to fit the uncorrected signal to a Lorentzian generally resulted in a very poor fit and an error of as much as 15% in the width.

It is well known that at moderate densities, coherent multiple photon scattering narrows the measured Hanle-effect linewidth.[9] Measurements were taken over an order-of-magnitude relative ion density to look for coherence narrowing. In the ion

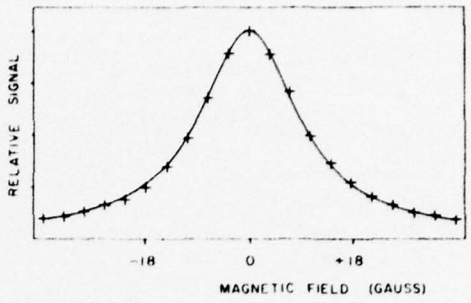

FIG. 1. Computer fit to Lorentzian of the $^2P_{3/2}$ Sr II Hanle signal.

density region of our experiment, less than 10^{10} cm^{-3}, coherence narrowing was not observed within experimental error. After coherence narrowing was determined to be negligible, attention was turned to collisional depolarization.[10] The collisional depolarization effect can be described by the equation

$$1/\tau = 1/\tau_0 + n\sigma v \ ,$$

where τ_0 is the true radiative lifetime, n is the helium density, σ is the alignment depolarization cross section, and v is the relative collisional velocity. When the collisional depolarization term $n\sigma v$ is not very much smaller than the radiative decay constant $1/\tau_0$, the collisional term must be eliminated by extrapolation to zero helium density. Figure 2 shows such a plot for the Sr II $^2P_{3/2}$.

Since Ba and Cd have a relatively high percentage of odd isotopes in natural abundance, it was deemed necessary to calculate their effect on the Hanle signal linewidth. The calculation was carried out

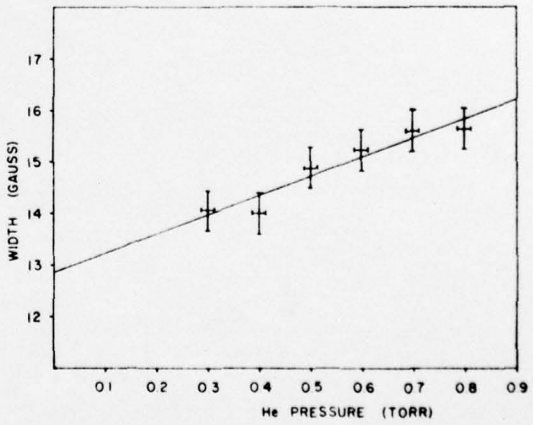

FIG. 2. Extrapolation to zero helium pressure. Data shown is for Sr II $^2P_{3/2}$ Hanle signal.

TABLE I. Radiative lifetimes of some group II $^2P_3$ ions.

Element	Configuration	τ (10^{-9} sec) This work	σ (10^{-15} cm^2) This work	τ (10^{-9} sec) Other work
Mg	$3p$	3.65(0.12)	5.65(2.8)	3.67(0.18) [a]
Ca	$4p$	6.61(0.30)	10(2.8)	6.72(0.2) [a]
Zn	$4p$	2.4(0.3)	---	3.0(0.3) [b] 3.1(0.4) [c]
Sr	$5p$	6.64(0.19)	9.5(1.6)	6.53(0.20) [a] 5.63(0.17) [d]
Cd	$5p$	2.86(0.25)	---	2.6(0.2) [e] 3.4(0.4) [b] 3.4(0.7) [c]
Ba	$6p$	6.78(0.40)	19(6)	6.27(0.25) [a] 7.0(0.6) [f]

[a] Lifetime by Hanle effect. References 2 and 3.

[b] Lifetime by beam-foil technique. T. Anderson and G. Sorensen, J. Quant. Spectrosc. Radiat. Transfer 13, 369 (1972).

[c] Lifetime by phase-shift technique. S. R. Bauman and W. H. Smith, J. Opt. Soc. Am. 60, 345 (1970).

[d] Lifetime by Hanle effect. Reference 6.

[e] Lifetime by the Hanle effect. Reference 13.

[f] Lifetime by Hanle effect. H. Bucka, J. Eichler, and G. V. Oppen, Z. Naturforsch. 21, 654 (1966).

in the same manner as described in detail in Ref. 7. The effect is estimated to be no more than a 2% broadening for Ba and 3% broadening for Cd. Isotope effects in the other materials will be insignificant because of the low natural abundance.[3] We have chosen not to incorporate the hyperfine effect into the lifetimes, but rather state it as an added uncertainty.

EXPERIMENTAL RESULTS

Table I is a compilation of our results along with those of other authors. Our data represent the first lifetime measurements in a flowing helium afterglow on group II ions. Here, by a single technique in a single apparatus, we present radiative lifetimes for six group II ions in the $^2P_{3/2}$ state. Any systematic error would therefore be expected to appear in all measurements. Error bars given in the data are always greater than rms scatter and should at least partially compensate for any systematic error.

Our data are in extremely good agreement with that of Gallagher and Smith. Interestingly enough, the only significant disagreement with their data is the Ba II lifetime, which is closer to the value of Bucka[11] *et al*. There is significant disagreement between Kelly's value for the Sr II lifetime, and that of Gallagher and our own. Our greatest source of experimental error was from the ion background field dependence, as described previously. Had we not corrected for this effect, our measured lifetime would have been about 5.7 nsec,[12] very near Kelly's 5.63. Unfortunately, we could not test Kelly's claim of high depolarization cross section from collisions with neutral Sr since our neutral density were so low ($\leq 10^{12}$ cm^{-3}). His value for the depolarization cross section of 8.4×10^{-13} cm^2, even though large, would have an insignificant effect on our measured lifetime.

Our lifetimes for Zn II and Cd II $^2P_{3/2}$ levels are consistently 15% shorter than measurements by beam-foil and phase-shift techniques. Hamel and Barrat[13] have measured the lifetime of Cd II by the Hanle effect in a dc discharge with He as the buffer gas. Our lifetimes agree with theirs to within experimental error. They also report a depolarization cross section with He of 4.6×10^{-15} cm^2. At the low helium pressure of our experiment, this effect would be very small compared to the error bars. For the same reason, the depolarization cross section for Zn was not measured. From the other measurements it is expected to be $\leq 10^{-14}$ cm^2, and again would have negligible effect on our lifetime measurement, which was taken at about 0.2-Torr He compared to the 1–4 Torr range of Ref. 13.

The depolarization cross sections reported here have large experimental errors because the pressure range covered was too small for some of the small width/Torr slopes encountered when plotting width versus helium pressure. The values obtained here, however, do fall within the range predicted for ion-atom collisions.[3]

*This research was supported by ONR grant No. ONR-N00014-75C-0477.

[1]W. Hanle, Z. Phys. 30, 93 (1924).
[2]W. W. Smith and A. Gallagher, Phys. Rev. 145, 26 (1966).
[3]A. Gallagher, Phys. Rev. 157, 24 (1966).
[4]Yu. I. Ostroskii and N. K. Penkin, Opt. Spektrosk. 10, 8 (1960); 11, 565 (1961) [Opt. Spectroc. 10, 3 (1961); 11, 307 (1961)].
[5]C. H. Corliss and W. R. Bozman, U. S. Natl. Bur. Stand. Monograph No. 53 (1962).
[6]F. M. Kelly, T. K. Koh, and M. S. Mathur, Can. J. Phys. 52, 1438 (1974).
[7]F. H. K. Rambow and L. D. Schearer, Phys. Rev. A 11, 738 (1976).
[8]L. A. Riseberg and L. D. Schearer, IEEE J. Quant. Electron. QE-7, 40 (1971).
[9]E. B. Saloman and W. Happer, Phys. Rev. 144, 7 (1966).
[10]J. C. Hsieh and J. C. Baird, Phys. Rev. A 6, 141 (1972), and Ref. 3.
[11]H. Bucka, J. Eichler and V. Oppen, Z. Naturforsch. 21, 654 (1966).
[12]F. H. K. Rambow and L. D. Schearer, Bull. Am. Phys. Soc. 20, 1448 (1975).
[13]J. Hamel and J. P. Barrat, Optics Commun. 10, 331 (1974).

Reprinted from:

JOURNAL OF THE OPTICAL SOCIETY OF AMERICA VOLUME 65, NUMBER 11 NOVEMBER 1975

Rotational and predissociation lifetimes of the $A^2\Sigma^+$ state of OD*

David Wilcox, Richard Anderson, and Jerry Peacher

Department of Physics, University of Missouri, Rolla, Missouri 65401

(Received 7 May 1975)

The lifetime and predissociation probabilities of various rotational levels of the $A^2\Sigma^+$ state of OD were measured. A strong predissociation at $N' = 35$ was observed. This predissociation could be explained by the level crossing of the $A^2\Sigma^+$ state with the repulsive $^4\Sigma^-$ state which are mixed by a weak spin–orbit interaction.

Index Headings: Spectra; Deuterium.

In recent years there have been many lifetime measurements[1–11] of the $A^2\Sigma^+$ state of both OH and OD. The most comprehensive measurements were those Elmergreen and Smith,[1] Sutherland and Anderson,[2] and German.[3] Elmergreen and Smith measured the lifetime of various rotational levels of the $v' = 0$ level of the $A^2\Sigma^+$ state of both OH and OD. They noted a strong predissociation in both systems for high rotational levels. Sutherland and Anderson's study was similar to that of Elmergreen and Smith, but it was restricted to OH. German measured the lifetimes of only the lower rotational states of OH and OD. Each study involved a different experimental technique; in the regions where they overlapped, they were in close agreement. This work is a continuation of the study by Sutherland and Anderson, extended to the $A^2\Sigma^+$ state of OD.

EXPERIMENT

The rotational lifetimes of the $v' = 0$ and 1 levels of the $A^2\Sigma^+$ state of OD have been measured from $N' = 3$ to 42 for $v' = 0$ and $N' = 8$ to 25 for $v' = 1$. All lines were measured at five different D_2O pressures; the zero-pressure lifetime was extrapolated. The sample was ROC/RIC 99.8% D_2O. The D_2O was pumped upon for a long period of time to remove any gases that became dissolved in it during transfer. The D_2O was continuously flowed through the discharge; the pressure was controlled with a stainless-steel needle value; it was measured with a CVC thermocouple gauge calibrated against a Stokes mercury manometer.

The discharge was excited by a pulsed rf oscillator with an electrical cutoff time of 15 ns. This apparatus was described in the earlier paper.[2] The discharge dissociated the D_2O and excited the $A^2\Sigma^+$ state of OD in a pulsed fashion. A Spex 1500 $\frac{3}{4}$ m monochromator resolved the OD spectral lines; they were detected with a 6256S photomultiplier. In order to resolve the spin doublets, 10 μm slits were used for the (0, 0) band; 30 μm slits were required for the (1, 0) band because of the low intensity of the band. All spectral identifications are based on the spectrographic data of Clyne, Coxon, and Woon Fat.[12]

Lifetime data were obtained by use of the delayed-coincidence technique, which was described in the earlier paper.[2] This technique involves the use of a level discriminator, a time-to-pulse-height converter, and a multichannel analyzer, which was operated in the pulse-height mode. The same apparatus was used to scan the spectra, except that the multichannel analyzer was operated in the multiscale mode. The data were analyzed on an IBM 370 computer.

RESULTS AND DISCUSSION

Figure 1 is a typical observed spectrum. Figure 2 is a typical decay curve of an OD line; it is evident that there is a single exponential decay.

Table I is a comparison of the results of this study with the results of other investigators,[1,3,6–9] for the (0, 0) band. Figures 3 and 4 are the variations of lifetimes of transitions from various rotational levels of the $A^2\Sigma^+$ state for the two spin components of the (0, 0)

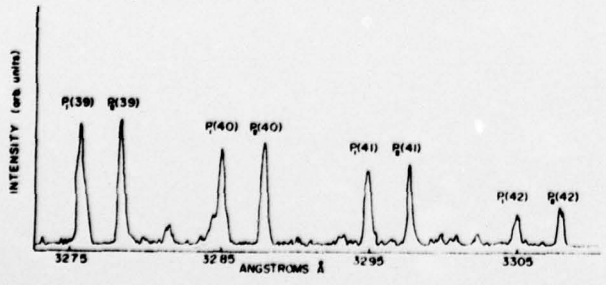

FIG. 1. OD spectrum near the last observable emission lines.

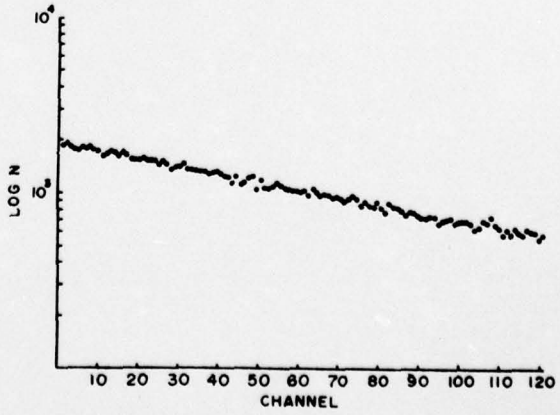

FIG. 2. Log plot of raw data from multichannel analyzer.

TABLE I. Comparison of results of studies of lifetimes in the (0,0) band of OD.

	Present study		Elmergreen *et al.* (Ref. 1)		German (Ref. 3)		German and Zare (Ref. 6)		deZafra *et al.* (Ref. 8)		German *et al.* (Ref. 9)	
N'	F_1	F_2	F_1	F_2	F_1	F_2	F_1	F_2	F_2	F_2	F_1	F_2
1					697 ± 7							
					691 ± 7	691 ± 7	630 ± 70				650 ± 60	
2			762 ± 80		689 ± 6	689 ± 6			598 ± 20			
3	790		762 ± 80									
4			762 ± 80		689 ± 8				598 ± 20			
5		760	762 ± 80									
6	761		754 ± 80									
7		760	754									
8			754	690	701 ± 8				598 ± 20			
9		812			711 ± 7							
10			740	722								
11	801		738 ± 80									
12	800											
13			790									
14				743								
15				752								
16				805								
17		780	760	744								
18		820	740	774								
19	803		770	790								
20	815	885	790	804								
21	785	820	723	793								
22	845	870	742	742								
23	877		800	805								
24	828		803									
25	810		793									
26	960	850	825	830								
27	910	960	855	875								
28		985	905	850								
29	1120	858	864	864								
30	1050	990	857	882								
31	875	980	834	886								
32	970	1080	870	870								
33	912	1108	880	920								
34	1106		985	970								
35	1080	900	985	950								
36	1050		985	940								
37			960	965								
38		1010	915	955								
39	937	640		950								
40	779			800								
41	490											
42		380										

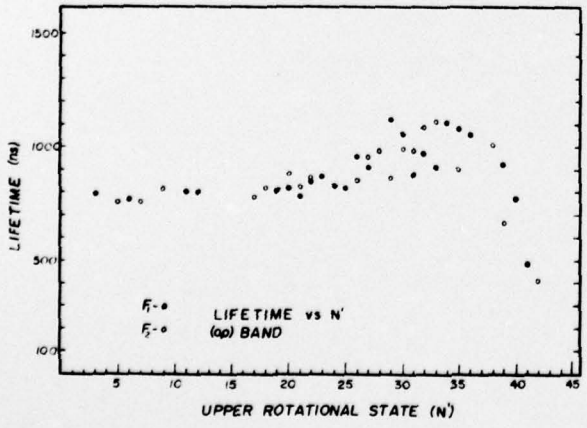

FIG. 3. Lifetimes vs N' for the OD (0,0) band.

and (1, 0) bands. For the (0, 0) band, the predissociation probabilities are given for each spin component in Table II.

The largest uncertainty in the lifetime measurements listed in Table I and Figure 3 for the (0, 0) band is 5%. Since the intensity of the (1, 0) band was weaker, the uncertainty is larger. In this case all measurements have an uncertainty less than 10%.

A strong predissociation is indicated by the shortening of the lifetime at $N' = 35$ for the (0, 0) band. The data indicate that the F_1 and F_2 spin components have nearly the same lifetime. A variation of the lifetime at $N' = 21$, 25, and 31 was observed. All of these results were observed by Elmergreen and Smith.[1]

The lines that arise from high rotational levels of the (1, 0) band were weak; therefore, their lifetimes

TABLE II. Predissociation probabilities for rotational levels for $N > 35$.

N'	F_1 (s^{-1})	F_2 (s^{-1})
36	0.0514×10^6	
37		
38		0.0891×10^6
39	0.1663×10^6	0.6616×10^6
40	0.3827×10^6	
41	1.1399×10^6	1.7306×10^6
42		

could not be measured. The expected predissociation, which should begin at $N' = 30$ or 31 for this system, could not be observed. For the (1, 0) band, a nearly constant lifetime was measured, whereas for the (0, 0) band, we found an increase with rotational level until predissociation began.

The lifetimes measured in this study are in close agreement with those of Elmergreen and Smith.[1] They are slightly greater than those reported by German.[3] In all studies, the lifetimes of the (0, 0) band increased with rotational quantum number until predissociation commenced. Our study was the only one that measured lifetimes for the (1, 0) band.

CONCLUSIONS

All three comprehensive studies on OD involved different experimental techniques; in the region where they overlapped, agreement was excellent. The same predissociation effects were observed in the (0, 0) band for levels above $N' = 35$. If the isotopic shifts of the energy levels are taken into account, the predissociation observed in OD is also caused by the crossing of the repulsive $^4\Sigma^-$ state and the $A^2\Sigma^+$ state. The transition between these forbidden states arises from the weak spin–orbit interaction, which mixes the states. This is the same effect as was observed for the $A^2\Sigma^+$ state of OH.[1,2]

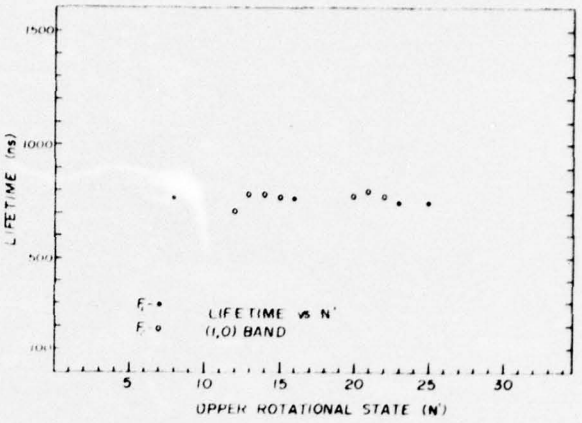

FIG. 4. Lifetimes vs N' for the OD (1, 0) band.

*This work was supported under the Office of Naval Research Contract No. N0004-14-75C-0477.

[1]B. G. Elmergreen and W. H. Smith, Astrophys. J. 178, 557 (1972).
[2]R. A. Sutherland and R. A. Anderson, J. Chem. Phys. 58, 1226 (1973).
[3]K. R. German, J. Chem. Phys. 62, 2584 (1975).
[4]R. G. Bennett and F. W. Dalby, J. Chem. Phys. 40, 1414 (1967).
[5]K. R. German and R. N. Zare, Phys. Rev. 186, 9 (1969).
[6]K. R. German and R. N. Zare, Bull. Am. Phys. Soc. 15, 82 (1970).
[7]W. H. Smith, J. Chem. Phys. 53, 792 (1970).
[8]R. L. deZafra, A. Marshall, and H. Metcalf, Phys. Rev. A3, 1557 (1971).
[9]K. R. German, T. H. Bergman, E. M. Weinstock, and R. N. Zare, J. Chem. Phys. 58, 4304 (1973).
[10]K. H. Becker, D. Haaks, and T. Tatarsczk, Chem. Phys. Lett. 25, 564 (1974).
[11]K. R. German and R. N. Zare, Phys. Rev. Lett. 23, 1207 (1969).
[12]M. A. A. Clyne, J. A. Coxon, and A. R. Woon Fat, J. Molec. Spectrosc. 46, 146 (1973).

Radiative lifetime of the $B\,^2\Sigma^-$ state of CH*

Richard A. Anderson, Jerry Peacher, and David M. Wilcox

Department of Physics, University of Missouri-Rolla, Rolla, Missouri 65401
(Received 29 August 1975)

The radiative lifetimes of the $N' = 3$ to 15 rotational states of the $v' = 0$ level of the $B\,^2\Sigma^-$ state of CH were measured. Emission lines were observed to $N' = 15$, but no lines above this rotational state were observed. This result agrees with previous studies. The lifetimes of all rotational states were between 300 and 400 ns. Previous measurements have indicated that the $N' = 15$ level might have a lifetime as short as 100 ns.

INTRODUCTION

Experimental and theoretical studies have shown that the $B\,^2\Sigma^-$ state of CH has a potential maximum.[1-5] Experimentally the emission spectrum[1] from the $v' = 0$ level of this state breaks off at $N' = 16$ and the broadening of absorption lines[2] occurs at $N' = 18$. Johns and Herzberg[2] predicted a maximum in the potential curve of the state from limiting curves of dissociation and the form of this potential maxium has been theoretically studied.[3-5]

Initial lifetime studies[6-9] only measure band head lifetime with instruments of low dispersion. Brooks and Smith[10] performed the first extensive study on this state. The lifetimes of the rotational levels to $N' = 15$ for $v' = 0$ and the $N' = 6$ for $v' = 1$ were observed.

Three theoretical studies[11-13] to predict the lifetime of the $B\,^2\Sigma^-$ state have been performed. In all of these studies only state lifetimes were calculated and not lifetimes for individual rotational levels.

The present experiment is similar to that of Brooks and Smith,[10] except that a different experimental technique was used. The delayed coincidence technique was employed so that actual decay curves of the excited levels could be observed. Many lines at shorter wavelengths could be described by single exponential decays and those at longer wavelengths exhibited two exponential decays. In the discussion of our paper this distinction will be important.

EXPERIMENTAL METHOD

The delayed coincidence method of single photon counting was used in conjunction with a pulsed rf discharge at 70 MHz with an electrical cutoff of 15 ns. The spectral lines were isolated by a Spex 1500 $\frac{3}{4}$ m monochromator with a 1500 lines/mm grating. The spectral lines were detected with an EMI 6256S photomultiplier. For the isolation of most spectral lines, a bandwidth of less than 0.3 Å was used. The output pulse of the photomultiplier was amplitude discriminated by an EG&G T200/N fast trigger and was timed by an Ortec 437 time to pulse height converter (TPHC). This output was stored in a Nuclear Data 1100 multichannel analyzer. The data were converted to paper tape and cards and read directly into an IBM 370 computer for analysis.

The methane (CH_4) used in the experiment was Matheson ultrahigh purity grade. The gas was flowed continuously through the discharge region. The pressure was controlled with a stainless steel needle valve and measured with a CVC thermocouple gauge calibrated against a Stokes mercury manometer.

For the time calibration of the TPHC and the multichannel analyzer two methods were used. In one case, a pulse was sent to the start of the TPHC and also through a cable of accurately known delay to the stop of the TPHC. Several different cables were used and counts were accumulated in the memory of the multichannel analyzer depending upon the time delay. In the second case, a start pulse from a HP 222 A pulse generator was used to start the TPHC and drive a Dumont 792 A pulse generator which had a variable delay. This delayed pulse stopped the TPHC. The delay times set on the pulse generator were measured on a HP 1710A oscilloscope which was time calibrated with a Tektronix 180-S1 time mark generator.

RESULTS AND DISCUSSION

A spectrum of the emission taken at high pressure is shown in Fig. 1. The long wavelength region of the spectrum was overlapped by a short lifetime component. This component is strongly quenched so that at high CH_4 pressures the spectrum is mainly that of CH. At low pressures the intensity of the short lived component can become equal to or slightly greater in intensity than the long lived components for some lines. These are the 3953, 3962, 3972, 3983, 3995, 4008, and 4021 Å lines.

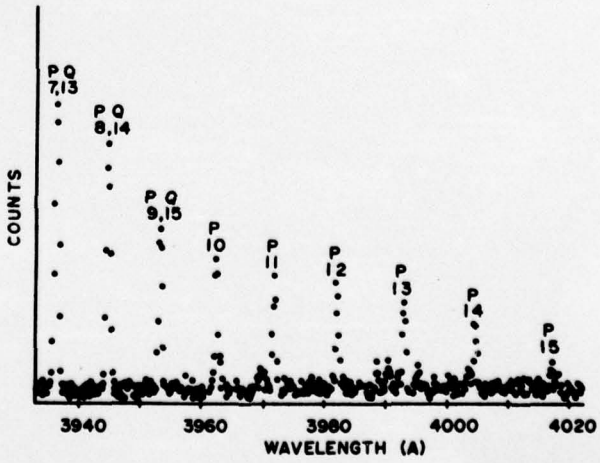

FIG. 1. A portion of the CH spectrum taken at high CH_4 pressures.

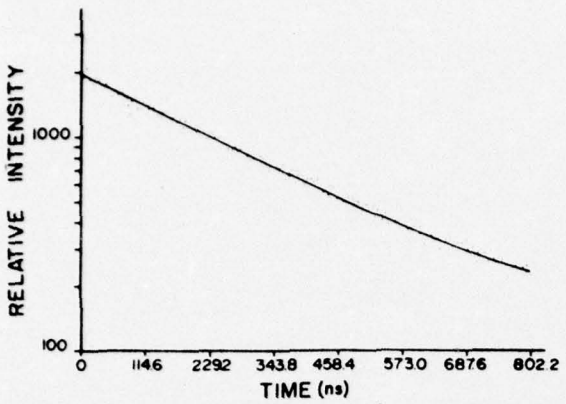

FIG. 2. The decay curve of the 3902 Å line at 30 mtorr and the computer fit.

TABLE I. Radiation lifetime of rotational states of the $v' = 0$ level of the $B^2\Sigma^-$ state of CH.

Upper state N'	Lifetime ns	Wavelength of transition Å
3	381 ± 18	3891
4	352 ± 24	3893
5	335 ± 10	3895
7	345 ± 23	3902
8	349 ± 8	3906
9	395 ± 21 (364 ± 24*)	3910 (3953*)$P(9)Q(15)$
10	345 ± 16	3916
11	368 ± 20	3972
12	405 ± 26	3983
13	399 ± 29	3995
14	430 ± 18	4008
15	416 ± 53 (364 ± 24*)	4021 (3953*)$P(9)Q(15)$

A typical decay curve for the 3902 Å line at 30 mtorr CH_4 pressure is shown in Fig. 2. The solid line is the computer fit to the curve. Data on all lines were taken at four or more CH_4 pressures. The 3902 Å line is nearly a single exponential decay. Most CH lines, which are not overlapped by the short lived component, are nearly pressure independent. CH lines overlapped by the strongly pressure dependent short lived component are more pressure dependent. This dependence is mainly caused by the fact that the computer cannot yield an entirely unique solution to an equation of the form $I = A\ \exp(-t/\tau_1) + B\exp(-t/\tau_2) + C$.

Lifetimes of the long decay component are shown in Fig. 3. These lifetimes were measured by examining lines where there was no overlap of other CH lines. Since the line arising from the $N' = 15$ level was weak, the overlapped $P(9)Q(15)$ line at 3953 Å was also examined. The lifetime (asterisk) for the 3953 Å line is shown opposite the nonoverlapped lifetimes for the $N' = 9$ and 15 levels. Table I shows the same results in tabular form.

The CH spectral lines were identified from the papers by Moore and Broida[14] and Bass and Broida.[15] In these papers the levels are designated by lower state rotational quantum numbers. Brooks and Smith[10] identified these as upper state quantum numbers. If only Q lines are examined, this makes no difference, but if P and R branch lines are included in their figures, the rotational quantum numbers may be mislabeled. The recent work by Botterud, Lofthus, and Veseth[16] on the term values of CH indicate that Moore and Broida[14] used lower state rotational quantum numbers.

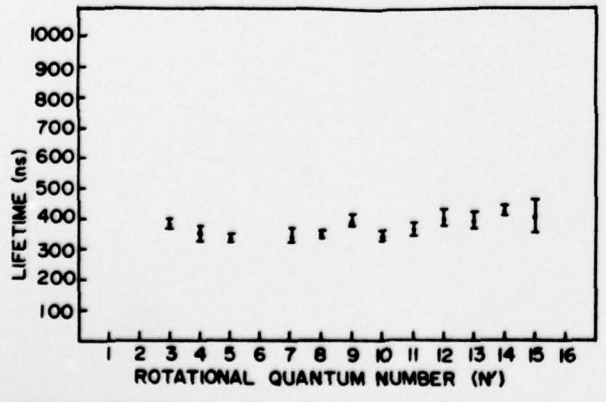

FIG. 3. The lifetimes of rotational states of the $v' = 0$ level of the $B^2\Sigma^-$ state of CH.

The most striking difference between our results and those of Brooks and Smith[10] is that the $N' = 15$ level does not shorten. The lifetime of the $N' = 15$ level was measured at 4021 Å corresponding to the $P(15)$ line[16] and the 3953 Å line was also examined corresponding to the $P(9)Q(15)$ line.[16] At 3953 Å the short lived component became apparent and for the lines between 3953 and 4021 Å the "zero pressure" short component lifetime was between 50 and 100 ns. This may have been the lifetime measured by Brooks and Smith.[10] Since this short component lifetime was evident for all lines above 3953 Å, it could not be identified as the shortened lifetime of the $N' = 15$ state. It was probably caused by a background of H, H_2, and CH^*.[10] Since the background was intense and the $P(15)$ line was weak, the error for this line is larger than for the other lines, but the lifetime value observed in our experiment is close to the lifetime of all of all other CH lines and also the $P(9)Q(15)$ line at 3953 Å. All lifetimes listed in Table I are nonoverlapped CH lines except for the 3953 Å line which was measured for comparison with $P(15)$ line at 4021 Å.

When the emission spectra of CH are examined, the last line observed is the $P(15)$ line with the intensity of the lines gradually decreasing from the $P(8)Q(14)$ line at 3943 Å. The $P(16)$ line is not present and this agrees with earlier studies.[1] From this study the $N' = 16$ level of CH is the first level tunneling through the potential barrier and has a lifetime so short that it cannot be measured. Since all CH levels from $N' = 3$ to 15 have the same lifetime, they are all visible but may have gradually decreasing intensities beyond $N' = 8$, and the $N' = 16$ level is not apparent because of its rapid tunneling through the potential barrier. This rapid tunneling also accounts for the broadening of the $N' = 18$ level in absorption.[2] Since the absorption line ending on the $N' = 18$ level is broadened and the true predisso-

ciation limit can best be determined by the break-off of an emission series, the $P(16)$ line first shows predissociation and the $N' = 16$ level can have a lifetime 10 100, or more times less than the $N' = 15$ level.

From these results the barrier height of the $B\,^2\Sigma^-$ state must be greater than 700 cm^{-1} using the data of Herzberg and Johns[2] and Botterud, Lofthus, and Veseth.[16] This result is also in close agreement with the results of Herzberg and Johns[2] and Lee, Hinze, and Liu,[3] which are greater than 500 and 800 cm^{-1}, respectively.

CONCLUSION

In conclusion, the lifetime of all rotational states from $N' = 3$ to 15 are nearly the same with a slight increase in lifetime with the rotational quantum number. The $P(16)$ line does not appear and the $N' = 16$ level has a lifetime so short that the line arising from it is not seen. This result agrees with the observation of emission spectra and the broadening of the $N' = 18$ level in absorption. This result combined with new determinations fo term values[16] yields a potential maximum greater than 700 cm^{-1}.

*This research was supported by the Office of Naval Research Contract No. N00014-69-A-0141-004.

[1]T. Shidei, Japan J. Phys. 11, 23 (1936).
[2]G. Herzberg and J. W. C. Johns, Ap. J. 158, 399 (1969).
[3]G. C. Lie, J. Hinze, and B. Liu, J. Chem. Phys. 59, 1872 (1973).
[4]P. S. Julienne and M. Krauss, *Molecules in the Galactic Environments* (Wiley, New York, 1973), p. 353.
[5]G. C. Lie, J. Hinze, and B. Liu, J. Chem. Phys. 57, 625 (1972).
[6]R. G. Bennett and F. W. Dalby, J. Chem. Phys. 32, 1716 (1960).
[7]E. H. Fink and K. H. Welge, J. Chem. Phys. 46, 4315 (1967).
[8]J. E. Hesser and B. L. Lutz, Ap. J. 159, 703 (1970).
[9]R. A. Anderson, D. M. Wilcox, and R. A. Sutherland, Nucl. Instrum. Methods 110, 167 (1973).
[10]N. H. Brooks and Wm. Hayden Smith, Ap. J. 194, 513 (1974).
[11]A. C. Hurley, Proc. R. Soc. London A 249, 402 (1959).
[12]W. M. Huo, J. Chem. Phys. 49, 1482 (1968).
[13]J. Hinze, G. C. Lie, and B. Liu (private communication).
[14]C. M. Moore and H. P. Broida, J. Res. Natl. Bur. Stand. A 63, 19 (1959).
[15]A. M. Bass and H. P. Broida, NBS Monogram 24, U. S. Government Printing Office, Washington, D.C. (1961).
[16]I. Botterud, A. Lofthus, and L. Veseth, Physica Scripta 8, 218 (1973).